Twin laws and energy in monoclinic Hydroxyapatite, Ca5(PO4)3(OH)

AQUILANO D., BRUNO M., RUBBO M., PASTERO L., MASSARO F. R.
Twin laws and energy in monoclinic Hydroxyapatite, Ca5(PO4)3(OH)
CRYSTAL GROWTH & DESIGN (2015) 15
DOI: 10.1021/cg501490e

Twin laws and energy in monoclinic Hydroxyapatite, $Ca_5(PO_4)_3(OH)$

Dino Aquilano,[1] Marco Bruno,[1] Marco Rubbo,[1] Linda Pastero,[1] Francesco Roberto Massaro[2]

[1] *Dipartimento di Scienze della Terra, Università degli Studi di Torino, via Valperga Caluso 35, I-10125, Torino, Italy*
[2] *Dipartimento di Geoscienze, Università degli Studi di Padova, Via Gradenigo 6, I-35131, Padova, Italy*

*corresponding author: dino.aquilano@unito.it

Abstract

The most frequent twin law of the monoclinic Hydroxyapatite crystal (HAp, S.G.: $P2_1/c$) is examined from both geometrical and reticular point of view. The A_3 twin axis, parallel to the screw diad axis of the parent (P) crystal, generates two twinned (T) individuals, mutually rotated by 120°. The structure of the resulting twinned interfaces are hypothesized, following the Hartman-Perdok method for determining the most stable surface profiles. The twin energy for each interface, evaluated by *ab initio* calculation, indicates that the activation energy for the nucleation of a 3D twin can be hardly distinguished from the one needed to nucleate a single 3D crystal. Moreover, a triple monoclinic twin simulates the structure of a trigonal-hexagonal HAp single crystal and the growth morphology of a monoclinic twin gradually approaches the hexagonal habit as much as the twin grooves disappear during growth.

1. Introduction

Recently, we determined by means of ab initio quantum-mechanical calculation the athermal equilibrium shape of the monoclinic $Ca_5(PO_4)_3(OH)$ Hydroxyapatite (HAp hereinafter; space group $P2_1/c$; a_0=9.3253, b_0=6.9503, $c_0 \cong 2\times a_0$= 18.6436 Å; β=119.972°) and hypothesized that twinning of the low symmetry polymorph could "simulate" both structure and morphology of the higher symmetry hexagonal one.[1]

Apatite twinning is a controversial problem from both geometrical and reticular point of view; further, twin energy has never been evaluated, either for monoclinic or hexagonal polymorph. The first finding of natural apatite twin was reported more than one century ago.[2] At the time, only goniometric and optical data were available: apatite was considered belonging to the hexagonal symmetry and the only twin was described as cruciform one (penetration twin) with twin plane

$11\bar{2}1$. As it will be shown, to identify the polymorph it is not easy and often it helps to consider both possibilities (monoclinic, hexagonal). Then, from now on, we will outline the hexagonal indexing and the corresponding monoclinic one; for the sake of uniformity with our preceding paper the space group $P2_1/c$ is adopted for the monoclinic frame. In this case, being $11\bar{2}1_{hex} \rightarrow 112_{mono}$, the composition plane of the cruciform twin does not correspond to a form belonging to the equilibrium shape of the crystal.[1] Much later,[3] three other twin laws were reported for apatite crystals morphologically belonging to the hexagonal symmetry. The new twin planes were: $10\bar{1}3$, $11\bar{2}3$ and $10\bar{1}0$, corresponding to 032, 132 and 001 planes in our monoclinic frame, respectively. It is worth outlining that $11\bar{2}1$, $10\bar{1}3$ and $11\bar{2}3$ twin planes, belong to pyramidal forms, and then parent (P) and twinned (T) individuals can be unambiguously distinguished. On the contrary, $10\bar{1}0$ twin plane belongs to the most important prism of the hexagonal phase; this implies that the two (more) individuals building a simple (multiple) twin share the same direction ($[001]_{hex}$ axis) and then it can be easily taken for a parallel association of crystals, all having the same orientation of their lattice frames.

Literature about apatite twinning underwent a sensible shift after the discovering of the monoclinic polymorph in pure and stoichiometric Chloro-apatite (ClAp) and HAp,[4,5] and in ClAp twins.**[6]** In a milestone paper on apatite twinning,[6] Prener showed that ClAp crystals, optically examined under crossed polarizers, were multiple twinned: in other words, three interpenetrating twins grew oriented 120° each other, all having in common the c_0 axis of the monoclinic structure (space group $P2_1/b$, as it ensues from the absence of odd *k*-indexes in *hk0* and odd *l*-indexes in *00l* X-ray reflections). Owing to the doubling of the b_0 cell parameter ($b_0=2a_0$) in the monoclinic polymorph, the multiple twinning resulted in the growth of mimetic twins having apparent hexagonal symmetry. Accordingly, the twin planes were 120 and $1\bar{2}0$.[6] Elliott confirmed**[7]** that the diffraction pattern of HAp crystals he prepared, exhibited "extra reflections" explicable on the basis of the space group $P2_1/b$ and the presence of mimetic twinning; this is commonly observed also in ClAp crystals having that space group.[8] Following Elliott et al.,[9] one should consider that the twin operation is a 120° rotation (clock and/or anticlockwise twin axis A_3) about the pseudo-hexagonal c_0 axis ($b_0=2a_0=18.84$Å; $c_0=6.88$Å; $\gamma=120°$); further, none of the more than ten specimen examined was free of twinning. Twin occurrence is also usually observed in ClAp rare-earth elements (REE)-doped: all crystals investigated by Fleet et al.,[10] are mimetic, with twinned individuals related by 120° rotation, in analogy with the just quoted findings.[8,9] Moreover, the twinned diffraction pattern has hexagonal symmetry.

Let's now propose a summarizing comment: independently of the just quoted twin laws (twin axis, twin plane), all monoclinic twins share a common direction (the A_2 diad axis of the structure), which coincides with the [001] axis of the hexagonal polymorph. On the other hand, it is difficult to obtain the pure monoclinic phase, as shown by Elliott et al.[9] who produced "… a specimen 63% hexagonal and 37% monoclinic…"; moreover, the hexagonal to monoclinic ratio varies from specimen to specimen in the same crystallization batch;[11] finally, twin free monoclinic crystals are quite rare.[12] Concluding, one can remark that there are good chances to confuse twins of monoclinic apatite with the twins of the hexagonal polymorph. The following examples will allow a deeper insight in such a complex situation.

Growth twinning was found as well in double REE substituted (Ce, Dy)-FAp and (Eu, Lu)-FAp crystals:[13] twin individuals have space group $P6_3/m$ and are mutually related by a 180° rotation about the [001] axis.

Crystal structure of twinned Cadmium Chlorapatite, $Cd_5(PO_4)_3Cl$, was investigated in two sound papers by the Donnay's School.[14,15] Crystals A and B building the twin by merohedry were attributed to the space group $P6_3/m$ and the twin operation was assigned, at a first moment,[14] either to the $10\bar{1}0$ or to $11\bar{2}0$ mirror plane, owing to the fact that symmetry reflections in both twin planes produce the same overlapping of X-ray peaks (because the coordinate axes of crystal B are symmetrical to those of crystal A). Successively,[15] the $11\bar{2}0$ twin law was ruled out because it requires too short interatomic distances across the expected twin composition surfaces. After recollecting the considerations mentioned about twinning by merohedry in Ca-apatites as "reported" in Dana's System of Mineralogy,[3] the authors concluded that $10\bar{1}0$ twinning by merohedry is doubtful or unconfirmed; further, they didn't observe it either in any of the tens of samples of $Ca_5(PO_4)_3F$, $Ca_5(PO_4)_3Cl$ and $Ca_5(PO_4)_3OH$, while twinning by merohedry of $Cd_5(PO_4)_3Cl$ was found everywhere in laboratory samples. Finally, comparing the structure of $Cd_5(PO_4)_3Cl$ with that of $Ca_5(PO_4)_3F$, a reason was found why "…twinning by merohedry is less frequent, perhaps absent…" in the latter; the factor hindering the twin formation in $Ca_5(PO_4)_3F$ was attributed to "…the physical accommodation of atomic positions and coordination across the original composition surface (OCS) of the twin". As a matter of fact, the required space is sensibly larger in the Ca-apatites than in Cd-chlorapatite.

Summing up, in this couple of papers one can find the first attempt to discuss not only the twinning of apatites in terms of lattice geometry, but also the structure of the possible twin interfaces in terms of bond energy.

The occurrence in apatites of the $10\bar{1}0$ twin law by merohedry was reconsidered very recently by Mills et al.,[16] who described "…the first documented case of $10\bar{1}0$ twinning by reflection…" in a

natural twin of Pyromorphite, $Pb_5(PO_4)_3Cl$. From single crystal X-ray diffraction were determined the space group $P6_3/m$, the cell parameters (a_0=10.0017 Å, c_0=7.3413 Å) and the approximate twin fraction (62:38). Two facts are quite surprising in this finding:

i) The first one concerns the morphology of the observed twin, made by only 6 faces, belonging to the following forms: two hexagonal prisms, $\{11\bar{2}0\}$ and $\{10\bar{1}0\}$, the pinacoid {0001} and two bi-pyramids, $\{10\bar{1}\,\bar{2}\}$ and $\{\bar{1}01\bar{2}\}$. In a single crystal this could correspond to a total of 38 faces; even if one accepts that the twin growth on the $\{10\bar{1}0\}$ composition plane halves the number of faces in zone with the [010] axis, the minimum number of faces limiting the twin would be 21, which is much larger than 6.

ii) The Authors state that the observed $\{10\bar{1}0\}$ twinning operation by reflection is equivalent to the twofold rotation about [100]. This is openly wrong, since the action of the symmetry center (due to the space group $P6_3/m$) on the twin $10\bar{1}0$ plane, generates the rotation axis [210].

When concluding, both remarks i) and ii) open to doubt the reliability of $10\bar{1}0$ twin law by merohedry in Pyromorphite.

The most complete work on growth morphology, polymorphism and twinning of apatite was likely made by Akizuki and coworkers 20 years ago,[17] on a natural sample having chemical composition $Ca_5(PO_4)_3$ $(F_{0.64},OH_{0.38},Cl_{0.01})$. The crystal morphology consisted of the {0001} pinacoid and of the hexagonal principal prism $\{10\bar{1}0\}$. From the interference contrast microscopy on the {0001} faces and from the optical examination between crossed polarizers of a 0001 thin section, it followed that the as grown {0001} surfaces were populated by minute growth hillocks, each of them limited by six $\{10\bar{1}l\}$ vicinal facets. The thin section showed, in the crystal bulk, fine *twinned six-fold sectors*; their shape was similar to that of the growth hillocks and, from this correspondence it ensued that "… the bulk texture of the crystal was produced during crystal growth, and not by alteration or transition in solid state after growth".

Measured variations of the 2V angle across the same 0001 thin section showed as well that the core of the crystal (belonging to the {0001} growth sector) is essentially monoclinic, while the crystal rim (belonging to the pseudo-hexagonal $\{10\bar{1}0\}$ growth sector) contains growth bands which are clearly uniaxial and then their structure is hexagonal. This proved, for the first time, that when investigating the surface patterns and the bulk features of a natural apatite crystal showing a hexagonal prismatic morphology, one can find that:

i) A perfectly hexagonal external crystal shape disguises a complex growth story in which the monoclinic polymorph largely dominated, since the initial stage of nucleation.

ii) The monoclinic polymorph, in turn, shows a fairly disturbed aspect, since this phase is not represented by a single crystal, but by a fine twinned texture composed by small growth domains, each of them showing pseudo-hexagonal symmetry.

iii) The final stage of growth is characterized by the overgrowth of un-twinned monoclinic polymorph ($2V_\alpha = 55°$), while in the second last stage the crystal shows the hexagonal structure ($2V_\alpha = 0°$). It is worth outlining that the prismatic profile corresponding to the hexagonal structure is composed not only by the faces of the primary $\{10\bar{1}0\}$ prism but also by those of the secondary $\{11\bar{2}0\}$ one.

Even if the thermal path of this natural sample and the composition of the growth medium and its variation, if any, are unknown, these observations suggest that the supersaturation should play a determining role in both polymorphism and twinning of apatite. As a matter of fact, one can reasonably hypothesize that the initial nucleation stage is characterized by highest level of supersaturation which progressively decreases until crystal stops growing. This would explain why multiple twinning of the monoclinic polymorph nucleated at the beginning of the crystallization while the hexagonal phase and the un-twinned monoclinic one appeared at the end of the crystallization.

Our research aims at determining the energy involved in apatite twinning. The main reason is obvious, i.e. the twin energy is the only parameter which determines, for a given supersaturation of the mother phase, the occurrence frequency of a given geometrical and structural twin law; in other words, it is the energy that rules both crystal structure and morphology and not vice versa. According to what we anticipated in the preceding paper,[1] here we confine our attention to the A_3 twin law of the monoclinic polymorph, which generates an individual (T) with respect to the (P) one, resulting in a parallel pseudo-hexagonal association of crystals. Peculiar care will be dedicated to rank the possible P/T interfaces and their configurations according to the twin energies and to evaluate the role of the twinning in the monoclinic $\leftrightarrow$ hexagonal transition.

There is another valid reason for studying the consequences of the A_3 twin law on the crystal habit of HAp when it crystallizes in the presence of specific impurities playing a fundamental role in biomineralization. As a matter of fact, the platy shape of HAp plays a fundamental role in determining the unique functional properties of bones[18] and the citrate ion is known to be adsorbed onto the prismatic HAp surfaces, so introducing a strong anisotropy in the HAp growth morphology which is supposed to be hexagonal when growing from pure aqueous solutions.[19] Recently, an interesting pathway has been proposed by Gomez-Morales and coworkers[20] to explain the "breaking of the hexagonal crystal symmetry" due to the HAp platelets which do not develop normal to the [001] axis of the space group $P6_3/m$. All that outlines once more the importance of the HAp

surfaces exposed to the mother phase during growth; the A_3 twin law of the monoclinic polymorph changes both the number of crystal forms and the ratio of their areas with respect to those exhibited by a single crystal. Therefore untwinned and twinned HAp crystals are reasonably supposed to differently behave when growing in the presence of impurities which are specific and strategic in biomineralization.

2. Computational details

To investigate the twin boundaries, a 2D periodic slab model[21] and the *ab initio* CRYSTAL09 code[22-24] were adopted. The calculations were performed by using the B3LYP Hamiltonian,[25-27] which provided accurate results for the surface properties of hydroxyapatite.[1] Further computational details (e.g., basis set, thresholds controlling the accuracy of the calculations) are reported in the Supporting Information.

A composed (twinned) slab, made by a parent slab (P) and a twinned slab (T), was generated in the following way: (i) the slab P of a given thickness was made by cutting the bulk structure parallel to the *hkl* twin plane of interest; (ii) the slab T was made by applying the appropriate twin law to the atomic coordinates of the slab P; (iii) then, the twinned slab geometry (atomic coordinates and 2D cell parameters) was optimized by considering all the atoms free to move. For more details on the construction of the twinned slab see the paper by Bruno et al.[28]

The CRYSTAL09 output files, listing the optimized fractional coordinates and optimized 2D cell parameters of the twinned slabs, are freely available at http://mabruno.weebly.com/download).

The calculation was done by considering twinned slabs with thickness up to ~30 Å, which is sufficient to obtain an accurate description of the twin interfaces. The slab thickness is considered appropriate when the bulk-like properties are reproduced at the centre of the slabs P and T.

The twinning energy, γ_{TE} (mJ/m^2), is the excess energy required to form a unit area of the twin boundary interface and reads:

$$\gamma_{TE} = \frac{E_T - E_{NT}}{A} \qquad (1)$$

where E_T and E_{NT} are the energies of the optimized twinned and not twinned slabs, respectively, and A is the area of the surface unit cell. More details on the strategy to calculate this quantity are reported in Bruno et al.[28]

3. The choice among the interfaces of the monoclinic HAp twins

3.1. Building a HAp monoclinic twin according to an A_3 rotation twin axis parallel to [010]

We assumed the HAp monoclinic cell ($P2_1/c$), as quoted in the Introduction and in our preceding paper: a_0=9.3253, b_0=6.9503, $c_0 \cong 2\times a_0$=18.6436 Å; β=119.972°.[1]

According to the introductory observations, the simplest twin operation for the monoclinic polymorph is an axis A_3 (or A_6) parallel to the $2_1 \equiv y$ axis of the single crystal:

i) Let's imagine a crystal viewed along the $2_1 \equiv$ [010] direction. In Fig. 1 (top) a crystal A is represented. The three main pinacoidal faces are labeled ($\bar{1}02$)-green, (100)-red, (001)-blue, along with their symmetry equivalent ones.

ii) Crystal B is generated through a 120° anticlockwise rotation around [010]. This operation transforms the parent crystal A in the twinned crystal B. An alternative operation can occur: crystal C can be obtained through a successive anticlockwise rotation of 120° of crystal B (which is equivalent to a 120° clockwise rotation of crystal A).

iii) Now, one has to choose among the original composition faces (OCF) for the nucleation of a twin. Let's consider a twin made by the couple A and B. One can generate a twinned interface A/B through the coupling: $(100)_A$ /$(\bar{1}02)_B$ (Fig. 1, bottom left); besides, two alternatives occur: $(001)_A$ / $(100)_B$ (Fig. 1, bottom center) and $(\bar{1}02)_A$ /$(001)_B$ / (bottom right).

iv) Then, building a HAp twin through the $A_3 \equiv$[010] twin axis, means that three different A/B interfaces could be considered. Further, we show (in the main text and in the Supporting Information) that for each of these interfaces the interface profile is not unique, owing to the different terminations of the facing profiles of the OCFs building the twin.

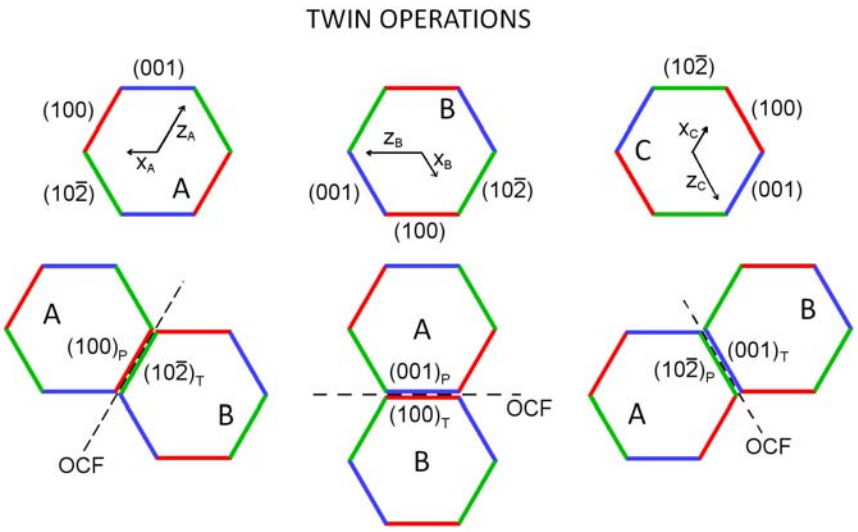

Figure 1. [010] projection of the monoclinic HAp equilibrium shape[1]. Top: twinned (T) crystals B and C are generated from parent (P) crystal A through 120° and 240° anticlockwise rotations, respectively (rotation axis A_3 ≡[010]), as indicated by the reference frames. Bottom: the three possibilities of generating an A_3 twin using the crystal couple A/B and the pinacoidal forms {001}, {100} and $\{10\bar{2}\}$ as original composition faces (OCF). Twinned couples A/C and B/C can be generated in the same way.

3.2. Building the interfaces of the monoclinic HAp twins

Considering now the growth aspect, a HAp twinned crystal can form if a 2D crystallite nucleates in twin position on the original composition faces (OCF) pertaining to the forms {010}, {001}, {100} and $\{10\bar{2}\}$. There are three couples of faces: (001), $(00\bar{1})$; (100), $(\bar{1}00)$; $(10\bar{2})$, $(\bar{1}02)$ which, all together, look like a pseudo-hexagonal prism and two pinacoidal ones: (010) and $(0\bar{1}0)$, as shown in Fig. 2.

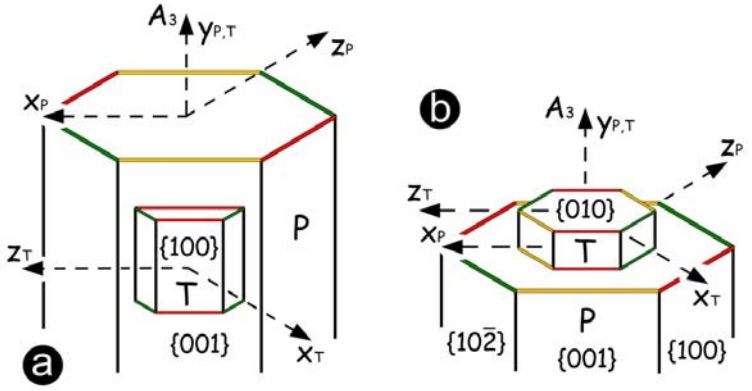

Figure 2. Two-dimensional twinned (T) nucleus forming on: (a) one of the {001} faces of the parent (P) crystal ; (b) one of the {010} faces of the parent (P). In both cases the twin operation is a rotation axis y ≡ A_3, as follows from the reference frames of P and T individuals. Different colors do identify different crystal forms.

A deep difference exists among the "prismatic" and the pinacoidal OCFs. First, we have to consider the coincidence lattices on the OCFs:

- The 2D coincidence cells (at the interface between the crystal P and the twinned nucleus T) are rectangular shaped for the "prismatic" OCFs, as one can see in Figs. 3a, b and c.
- The common 2D cell shows trigonal symmetry for the pinacoidal OCF (Fig. 3d)

Vectors defining the 2D coincidence meshes are detailed in Table 1.

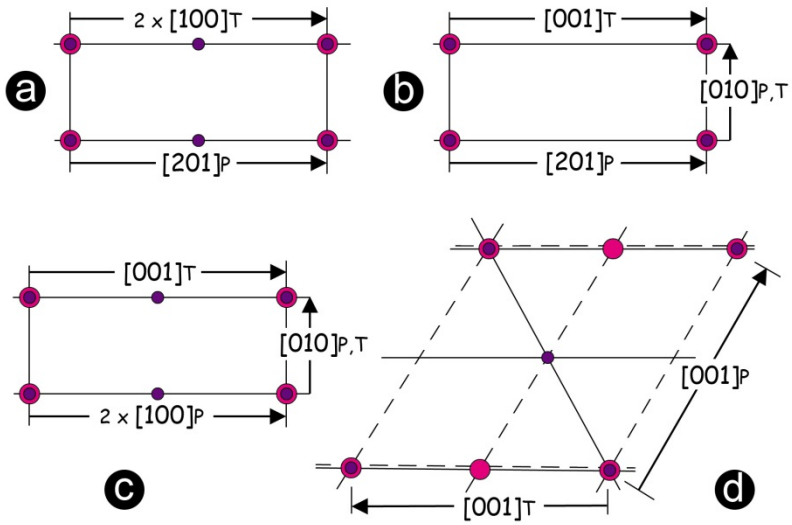

Figure 3. The 2D coincidence cells (at the P/T interface) are rectangular shaped for the interfaces: $(\bar{1}02)_T/(001)_P$ (a); $(\bar{1}02)_T/(100)_P$ (b); $(100)_T/(001)_P$ (c) and triangular shaped for the $(010)_T/(010)_P$ interface (d). See Table 1 for the cell multiplicity.

Twin interface	OCF (T/P)	2D coincidence lattice vectors	Shape of the 2D cell	Area of the 2D cell (Å^2)	2D cell multiplicity
a	$(\bar{1}02)_T/(001)_P$	[201]×[010]	rectangular	129.658	2
b	$(\bar{1}02)_T/(100)_P$	[201]×[010]	rectangular	129.658	1
c	$(100)_T/(001)_P$	[001]×[010]	rectangular	129.579	2
d	$(010)_T/(010)_P$	$[001]_T\times[001]_P$	triangular	301.008	3

Table 1. Type of interfaces (*a*-*d*) between parent and twinned individuals (column 1); original composition faces, OCFs, involved in the twinning, along with the faces of the twinned (T) nucleus adhering on them (column 2); lattice vectors limiting the 2D-coincidence cell forming at the twin interface (column 3); shape of the 2D-coincidence cell, its area and multiplicity (columns 4, 5 and 6 respectively).

Secondly, the continuity across the twin interfaces, of the HAp periodic bond chains (PBCs),[1] has to be taken into account.

According to Fig. 4, one can verify the continuity of all the PBCs parallel to the 010 plane crossing the type *a*, *b*, and *c* interfaces (Table 1); further, where the transition between P/T crystals occurs, the number and kind of first neighbors is preserved. In other words, at the level of the "prismatic" OCFs the structural order of the twin interface is barely perturbed with respect to that of the single crystal, as it will be detailed in the forthcoming sections.

The *d*-$(010)_P/(010)_T$ interface is characterized by a more severe structural discontinuity since the …ABABAB… stacking of the elementary d_{020} layers (which alternate according to the screw 2_1 axis) is deeply perturbed by the action of the A_3 twin axis. As a matter of fact, a twinned 2D nucleus forming on the $(010)_P$ face with thickness d_{020} will result rotated by 120° with respect to the underlying one. Owing to this rotation, the [001] PBC of the outmost B layer of the parent crystal will interact with a PBC parallel to [100] running within the twinned 2D nucleus, so giving rise to a discontinuous sequence …ABABABC. Hence, first neighbors interactions are profoundly modified across this interface: the adhesion of the twinned 2D nucleus should be compromised and, consequently, the twin energy will be decidedly higher with respect to that of the preceding case.

This is the main reason why we will confine our attention to the three prismatic interfaces of the twin. In Table 2, the surface terminations of the three pinacoids parallel to the y axis are recollected, along with the values of the specific surface energies (γ) corresponding to their optimal configuration.[1]

Form	**Surface termination**	**γ (mJ/m^2)**
$\{10\bar{2}\}$	PO_4, Ca, OH	1515
	PO_4 only	1725
{100}	PO_4, Ca, OH	1525
	PO_4 only	1723
{001}	PO_4, Ca, OH	1546
	PO_4 only	1712

Table 2. The three pinacoids building the [010] zone of the equilibrium shape of the monoclinic HAp crystal. Hard interfaces (higher γ values) correspond to surface profiles built by PO_4 ions only. When the surface profile is built by the PO_4, Ca and OH ions (softer interfaces), the indicated γ value corresponds to the optimal surface configuration.[1]

4. Structure of the monoclinic interfaces parallel to the twin axis (y≡A_3) and related twin energies

According to Table 1, both the *a*-$(\bar{1}02)_T/(001)_P$ and *c*-$(100)_T/(001)_P$ interfaces share the (001) face and show the same 2D-cell multiplicity. Moreover, when these interfaces form, a peculiar orientation of the OH ions occurs. Let's consider, for instance, the *c*-$(100)_T/(001)_P$ interface (Fig. 4a): within the alternating d_{002} layers building the T individual, the OH are oriented either along the positive or negative direction of the *y* axis; on the contrary, within each of the $d_{\bar{1}02}$ (or d_{100}) slices building the parent (P), the OH ions are oriented up-down.[1] As a consequence, one out of two [100] PBCs undergoes a discontinuity when crossing the twin interface.

A different situation generates for the *b*-$(\bar{1}02)_T/(100)_P$ interface, where the multiplicity of its coincidence 2D-cell is half the preceding one and both the $d_{\bar{1}02}$ and d_{100} slices practically show the same structure. As a matter of fact, the ordering of the hydroxyl groups within both the slices d_{002} (P) and d_{002} (T), undergoes the up/down discontinuity when crossing the twin interface. (Fig. 4b).

Table 2 shows that the specific surface energy values of the $\{10\bar{2}\}$ and {100} forms are very similar, due to the closeness of their surface profiles:[1] hence, we limit our attention to the calculation of the twin energy of the *c*-$(100)_T/(001)_P$ and *b*-$(\bar{1}02)_P/(100)_T$ interfaces. For the *c*-interface, two different surface configurations have been considered (see Figure SI.1 of the Supporting Information) in order to find the lowest twin energy.

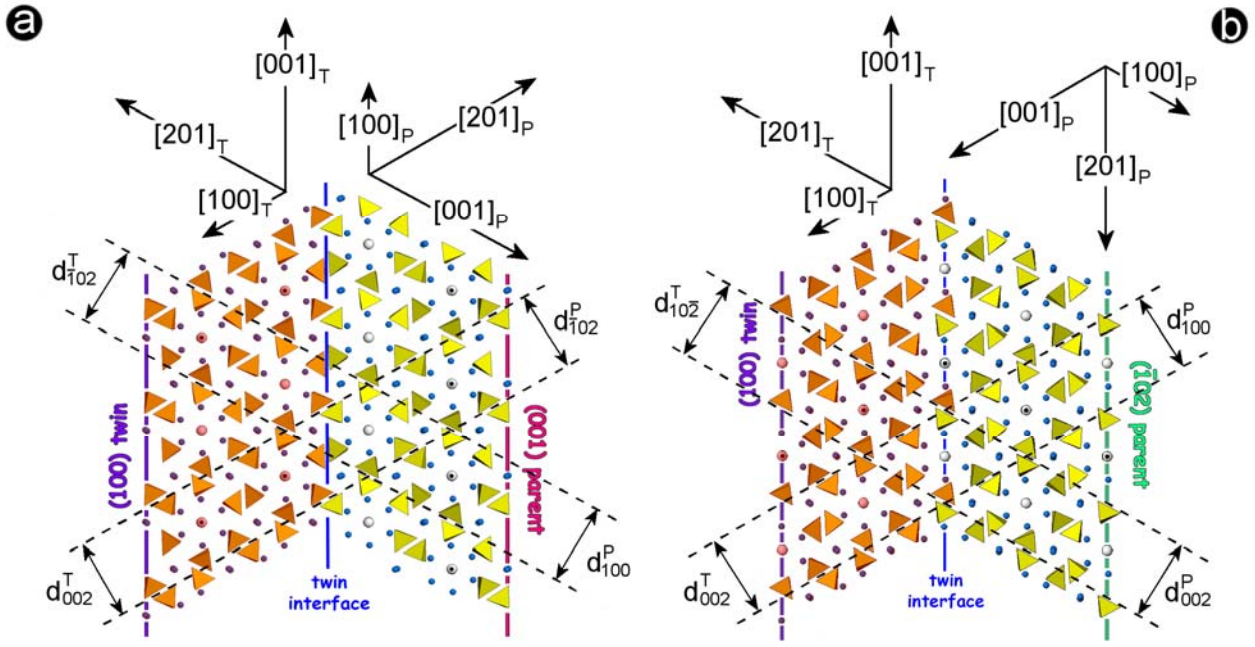

Figure 4. Projection along the $y \equiv$ [010] axis of a monoclinic HAp twin. P and T individuals are mutually rotated by 120° around the *y* axis: (a) The twin interface is composed by the original composition faces $(001)_P$ and $(100)_T$. Both P, T faces are terminated only by phosphate tetrahedra, according to one out of the choices allowed by the PBC analysis.[1] Across the twin interface the PBCs $[001]_P$ continue on the PBCs $[201]_T$ but the up/down sequence of the OH dipoles results to be interrupted at fifty per cent. Equally, the PBCs $[201]_P$ continue on the PBCs $[100]_T$ but all the up/down OH sequences of the P individual are interrupted at the twin interface. (b) The twin interface is composed by the original composition faces $(\bar{1}02)_P$ and $(100)_T$. Both P, T faces are terminated by one of the possible configurations made by PO_4, Ca and OH ions.[1] Contrarily to the case a), all the up/down OH sequences are interrupted in the same way by the twin interface. In both sides (a) and (b) the thicknesses of the elementary d_{h0l} layers allowed by the extinction rules are drawn, along with the reference frames of both P and T individuals.

Twin interface	**Interface configuration**	γ_{TE} **(mJ / m^2)**
c-$(100)_T/(001)_P$	PO_4 tetrahedra only	3.3
c-$(100)_T/(001)_P$	PO_4, Ca and OH ions	4.2
b-$(\bar{1}02)_T/(100)_P$	PO_4, Ca and OH ions	2.8

Table 3. The twin energy, γ_{TE}, of the monoclinic HAp, calculated for three original composition faces (OCF) in zone with the twin axis $A_3 \equiv y$.

From Table 3 it follows that the average of the twin energy values is less than 0.2% of the averaged value of the specific surface energy of the most important HAp forms (Table 2). Beyond the qualitative considerations we just made about the strong similarity between the structure of a HAp monoclinic single crystal and that of the rotation twins, this represents the quantitative evidence that the activation energies involved in the nucleation of single crystals and this type of twins are practically indistinguishable, at least when the twin OCFs are in zone with the twin axis. Moreover, it is reasonable expecting that the twin energy will maintain fairly low also when the OCF coincides with the {010} faces of both P and T individuals, as we will show in detail in a forthcoming paper.

5. A comparison between the experimental growth morphology of single crystals and A_3 twins of the monoclinic HAp

We obtained HAp crystals from hydrolyzed monetite ($CaHPO_4$), following a modified Perloff' s procedure.[29] Monetite, as a HAp precursor, was precipitated from a H_3PO_4 diluted solution saturated in $Ca_3(PO_4)_2$ at room temperature and then slightly heated up to close the boiling point. Monetite was hydrolyzed (monetite/water weight ratio 1/100) at 220°C (i.e. at a temperature lower than that used in the Perloff' s routine) and at an autogenic pressure in PFTE autoclaves for two weeks. Both monetite and HAp were obtained in CO_2 free atmosphere. After precipitation, HAp was filtered, dried at room temperature and then examined by XRPD and SEM. Detailed XRD study about the crystal structure of the product we precipitated is beyond the scope of the present work. Nevertheless, XRPD diagrams were carried out in order to: i) control that no Carbapatite was formed through accidental carbon dioxide contamination during growth; ii) ascertain that monoclinic HAp was the prevailing polymorph (either untwinned or twinned). To this purpose, the decomposition of the XRPD peak profiles has been applied in two strategic intervals of the XRPD patterns, as one can see in Supporting Information.

At low 2θ values (2θ≅11°), the peak shape clearly shows that, notwithstanding the low intensity of the diffracted signal, the peak profile is dispersed over a 2θ range which is larger than the calculated one for the pure monoclinic polymorph. At intermediate 2θ values, i.e.: between 30.6° and 33.3° , from the decomposition one can find at least six independent peaks, while only three should be expected from the pure hexagonal polymorph. All that reasonably proves that we have to do with a dominant monoclinic phase and that monoclinic twinning contributed to the reduction (from 15 to 6) of the number of peaks we could expected if the sample was composed by pure untwinned monoclinic individuals.

Figs. 5 and 6 allow to compare the experimental growth morphology we obtained for both single crystals and A_3 twins of the monoclinic HAp.

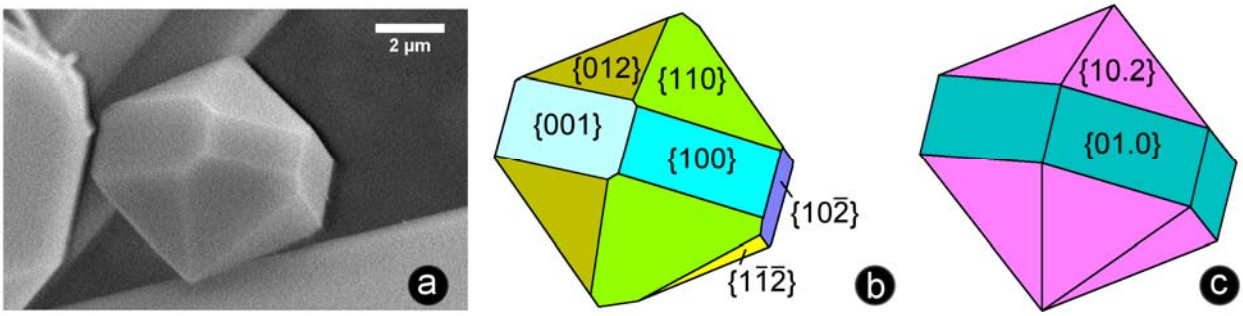

Figure 5 (a) SEM picture of our laboratory grown *monoclinic HAp single crystal* showing three adjacent and consecutive pinacoids: {001}, {100} and $\{10\bar{2}\}$, all parallel to the [010]≡A_2 zone axis, along with the corresponding prisms: {110}, $\{11\bar{2}\}$ and {012}. Theoretical growth morphologies simulating: (b) the monoclinic 2/m and (c) the hexagonal 6/m symmetry; different shades of color represent different crystallographic forms. The comparison outlines how the experimental HAp growth shape of the monoclinic polymorph could be easily confused with the hexagonal one.

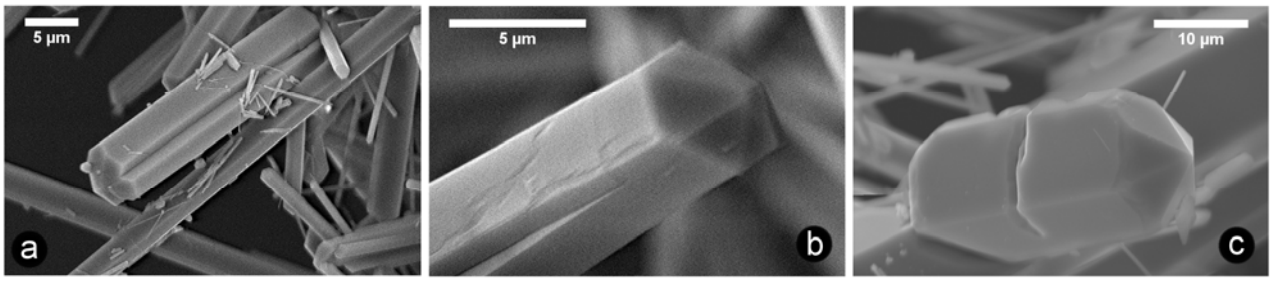

Figure 6. SEM picture of a monoclinic HAp twin: the original composition face of the twin can be one out of the pinacoids {100}, $\{10\bar{2}\}$ and {001}; the deep groove developing along the [010] axis proves that parent and twinned individuals are encompassing each other (a). As far as the twin continues growing, the groove vanishes and the twin tends to look like a single individual (b). While the twin law maintains unchanged, the original composition plane of the twin can vary: in (c) the residual groove witnesses for (010) as the original composition face.

The single crystal growth shape (Fig. 5a) is limited by three pinacoids: {100}, $\{10\bar{2}\}$ and {001}, all belonging to the zone axis [010]≡2_1, and by the corresponding prisms: {110}, $\{11\bar{2}\}$ and {012}. Compared to the theoretical equilibrium shape,[1] the crystal is not truncated by the basal pinacoid {010}; however, this is not surprising owing to the different kinetic behavior of the {010} form with respect to the other ones, as we have recently forecast[1] and as is illustrated in detail in Fig. SI.2 of the Supporting Information. The experimental growth shape and the simulated one (Figs. 5a and b) look a whole lot pseudo-hexagonal. This cannot be attributed to the strong closeness of the specific surface energies (γ) of the three pinacoids and of the three prisms, since γ represents an equilibrium property.[1]

Actually, the growth kinetics of the three pinacoids is determined by the total edge energy of the steps limiting the shape of the 2D nuclei which can be formed on their fresh surfaces; this, in turn,

depends on the structure of the PBCs lying within the elementary layers having thickness: d_{100}, $d_{10\bar{2}}$ and d_{002}. All these layers share the same [010] PBC and contain as well the PBCs [001], [201] and [100], respectively, which show practically the same structure.[1] Consequently, one can reasonably assume that the equilibrium shape and free energy of both the 2D nuclei and spiral exposed ledges should be the same for the three pinacoids.

Then, one cannot practically distinguish the growth kinetics of these forms, which can explain the pseudo-hexagonal symmetry of the HAp growth morphology. The same considerations hold true in the case of the prisms: {110}, {11$\bar{2}$} and {012}, and let to understand the crystal shape shown in Figs. 5a and b. Finally, Fig. 5c represents the simulated growth form of a hexagonal HAp crystal limited by a prism and the corresponding bi-pyramid.

Fig. 6a shows two monoclinic HAp individuals each other twinned according to the rotation A_3 twin axis ≡[010], as schematized in Fig. 1. One could object that we should have to do with a parallel association of iso-oriented single crystals simultaneously nucleated and adhering on the same pinacoidal face. But this is not the case for two reasons: a) Such an event is highly improbable, due to unfavorable balance of its activation energy for 3D nucleation; b) The presence of the groove developing all over the [010] direction indicates that the smaller individual nucleated after the bigger one and that the reciprocal encompassing during growth occurred preferentially on one out the two re-entrant dihedral angles limiting the original composition face; this lack of symmetry is typical of twins and not of the iso-oriented crystals

Fig. 6b shows that the groove of the twin tends to disappear, due to the concave dihedral angle effect[30] which accelerates the growth rate of the faces, forming the dihedral angle, with respect to the adjacent ones. Thus, it should be easy to foresee that the final aspect of this twin would be undistinguishable from that of a single individual.

Fig. 6c describes a HAp twin ruled by the same geometrical law of the preceding cases, i.e. the same rotation twin axis A_3≡[010]≡2_1 of the crystal. But, in this case, the original composition face is the {010} pinacoid. As a matter of fact, the residual groove which develops perpendicular to the [010] axis of the twin, witnesses that the nucleation mechanism of P and T individuals is that schematized in Fig. 2b. It is easy to forecast that also in this case the groove has to disappear during further growth, and that, once the filling of the dihedral angle is accomplished, the final look of the twin will be that of a single crystal.

6. Conclusions

We started from the reasonable doubts expressed by Donnay and co-woorkers[14,15] on the most frequent $(10\bar{1}0)$ twin law of Apatites and from the structural complexity of $(10\bar{1}0)$ twinned and hexagonally shaped crystals of natural samples of Hydroxy-fluorapatite qualitatively studied by Akizuki et al.[17] Convinced of the soundness of these works, and in order to put the investigation on a quantitative ground, we evaluated the energy excess needed to build a twin (i.e. the twin energy) of the monoclinic polymorph of pure HAp. The simplest and most frequent twin law has been chosen for our calculation, i.e. that generating a twinned (T) individual through a A_3 rotation axis parallel to the symmetry $[010] \equiv A_2$ axis of the monoclinic parent (P) crystal. Original composition faces (OCF) have been chosen according to their stability, as it is evident in the single crystal equilibrium morphology, and all possible twin interfaces have been hypothesized following the stability criterion determined in a preceding work.[1] Then, we calculated at *ab initio* level the corresponding twin energies and found that their values are three order of magnitude lower than the surface energy of the analogous faces (interfaces with vacuum) of the single crystal. This means that the supersaturation barrier to overcome for nucleating a 3D twin of monoclinic HAp (according to the investigated twin law) is nearly indistinguishable from that needed for a 3D single crystal. Such a conclusion explains, quantitatively, why twin free crystals of HAp and, more in general, of Apatites, are grown with difficulty and probably are rare in nature. Moreover, our SEM observations outline that the growth aspect of monoclinic HAp twins can be distinguished from that of a single monoclinic crystal just during the early stages of growth; but, as the growth progresses, the difference between twin and single crystal vanishes, owing to the filling of the twin grooves. Finally, a multiple (triple) twinning of a monoclinic individual could be optically distinguished from a hexagonal single crystal, since three biaxial crystals can never be confused with an uniaxial one; perhaps, when seen through the "eyes" of a X-ray beam, the set of three twinned individuals could assume the structure of a higher symmetry single crystal (an A_3 axis resulting from the quasi-perfect superposition of three reference frames mutually rotated by 120° around the [010] direction, as illustrated in Fig. SI.3 of the Supporting Information).

Summing up, our investigation proves once more that the path to sort out the dilemma: monoclinic/hexagonal? for HAp crystals can be successful only if X-ray diffractometric measurements are integrated with the optical determination of the birefringence and careful examination of the growth morphology.

Acknowledgments

The study was financially supported by MIUR−Ministero dell'Istruzione, Università e Ricerca; MIUR-Project PRIN 2010-2011, 2010EARRRZ_007: "Crystal-chemical and structural investigations on the bulk and surfaces of carbonated apatites with amorphous and nano-crystal transitions". We would like to thank the anonymous referees for valuable criticisms and useful suggestions that helped us to improve the quality of our present work.

Supporting Information: the two possible configurations of the twin interface when the original composition faces (OCF) are: $(001)_P$ and $(100)_T$ (Fig. SI.1); the disappearance of the {010} pinacoid from the growth morphology of HAp (Fig. SI.2). What do we will expect, as a final result, from two successive anticlockwise twin operations (with the A_3 rotation twin axis parallel to [010])? (Fig. SI.3). Computational details (SI.4). Decomposition of two XRPD diagrams of pure HAp (SI.5). This material is available free of charge via the Internet at http://pubs.acs.org.

References

(1) Aquilano, D.; Bruno, M.; Rubbo, M.; Massaro, F.R.; Pastero, L. *Cryst. Growth Des.* **2014**, *14,* 284.
(2) Palache, C.; Berman, H.; Frondel, C. *The Dana System of Mineralogy*, 6th ed. **1892**, *767*, New York.
(3) Palache, C.; Berman, H.; Frondel, C. *The Dana's System of Mineralogy*, 7th ed. Vol.II, (**1951**) p.*881*, New York: J. Wiley.
(4) Young R.A.; Elliot J.C. *Archs. Oral Biol.* **1966**, *11*, 699.
(5) Elliott , J.C.; Young, R.A. *Nature* **1967**, *214*, 904.
(6) Prener, J.S. *J. Electrochem. Soc: Solid State Science* **1967,** *114*, 77.
(7) Elliott, J.C. *Nature Physical Science* **1971**, *230*, 72.
(8) Mackie, P.E.; Elliott, J.C.; Young, R.A. *Acta Crystallogr.* **1972**, *B28*, 1840.
(9) Elliott, J.C.; Mackie, P.E.; Young, R.A. *Science, New Series* **1973**, *180(4090)*, 1055.
(10) Fleet, M.E.; Liu, X.; Pan, Y. *Amer. Mineral*. **2000** , *85*, 1437.
(11) Ikoma, T.; Yamazaki, A.; Nakamura, S.; Akao, M. *J. Solid State Chemistry* **1999**,*144*, 272.
(12) Suetsugu, Y.; Tanaka, J. *J. Mat. Sci. Mater. in Medecine* **2002**, *13,* 767.
(13) Fleet, M.E.; Pan, Y. *Amer. Mineral*. **1997**, *82*, 870.
(14) Sudarsanan, K.; Young, R.A.; Donnay, J.D.H. *Acta Crystallogr.* **1973**, *B29*, 808.
(15) Donnay, J.D.H.; Sudarsanan, K.; Young, R.A. *Acta Crystallogr.* **1973**, *B29*, 814.
(16) Mills, S.J.; Ferraris, G.; Kampf, A.R.; Favreau, G. *Amer. Mineral*. **2012**, *97*, 415.
(17) Akizuki, M.; Nisidoh, H.; Kudoh, Y.; T. Watanabe, T.; Kurata, K. *Mineral. Mag.* **1994**, *58*, 307.
(18) (a) Eppell, S.J.; Iong, W.; Katz, J.L.; Glimcher, M.J. *J.Orthop. Res*. **2011**, *19*, 1027. (b) Fratzl, P.; Gupta, H.S.; Paschalis, E.P.; Roshger, P. *J. Mater. Chem*. **2004**, *14*, 2115.

(19) (a) Filgueiras, M.R.T.; Mkhonto, D; De Leeuw, N.H. *J.Crystal Growth*, **2006**, *294*, 60; (b) Hu, Y.Y.; Rawal, A.; Schmidt-Rohr, K. *Proc. Nat. Acad. Sci. USA*, **2010**, *107*, 22425; (c) Xie, B.; Nancollas, G.H. *Proc. Nat. Acad. Sci. USA*, **2010**, *107*, 22369.
(20) (a) Delgado-López, J.M.; Frison, R.; Cervellino, A.; Gómez-Morales, J.; Guagliardi, A.; Masciocchi, N. *Adv. Functional Mater.* **2014**, *24*, 1090; (b) Iafisco, M.; Ramirez-Rodriguez, G.B.; Sakhno, Y.; Tampieri, A.; Martra, G.; Gómez-Morales, J.; Delgado-López, J.M. *CrystEngComm*. **2014**, doi: 10.1039/C4CE01415D.
(21) Dovesi, R.; Civalleri, B.; Orlando, R.; Roetti, C.; Saunders, V.R. In: Reviews in Computational Chemistry; Lipkowitz, B.K.; Larter, R.; Cundari, T.R., Eds.; John Wiley & Sons, Inc.: New York, 2005, vol.1, p.443.
(22) Dovesi, R.; Orlando, R.; Civalleri, B.; Roetti, C.; Saunders, V.R.; Zicovich-Wilson, C.M. *Z. Kristallogr.* **2005**, *220*, 571.
(23) Dovesi, R. *et al.*, *CRYSTAL09 User's Manual*; University of Torino: Torino, Italy, 2009.
(24) Pisani, C.; Dovesi, R.; Roetti, C. *Hartree-Fock ab-initio treatment of crystalline systems*, Lecture Notes in Chemistry; Springer: Berlin, Heidelberg, New York, 1988.
(25) Becke, A.D. *J. Chem. Phys.* **1993**, *98*, 5648.
(26) Lee, C.; Yang, W.; Parr, R.G. *Phys. Rev. B* **1998**, *37*, 785.
(27) Stephens, P.J.; Devlin, F.J.; Chabalowski, C.F.; Frisch, M.J. *J. Phys. Chem.* **1994**, *98*, 11623.
(28) Bruno, M.; Massaro, F.R.; Rubbo, M.; Prencipe, M.; Aquilano, D., *Cryst. Growth Des.* **2010**, *10*, 3102.
(29) Perloff, A.; Posner, A.S. *Science*, **1956**, *28,* 583.
(30) Boistelle, R.; Aquilano, D. *Acta Crystallogr.* **1978**, *A34*, 406.

For Table of Contents Use Only

Twin laws and energy in monoclinic Hydroxyapatite, $Ca_5(PO_4)_3(OH)$

Dino Aquilano,[1] Marco Bruno,[1] Marco Rubbo,[1] Linda Pastero,[1] Francesco Roberto Massaro[2]

[1] *Dipartimento di Scienze della Terra, Università degli Studi di Torino, via Valperga Caluso 35, I-10125, Torino, Italy*
[2] *Dipartimento di Geoscienze, Università degli Studi di Padova, Via Gradenigo 6, I-35131, Padova, Italy*

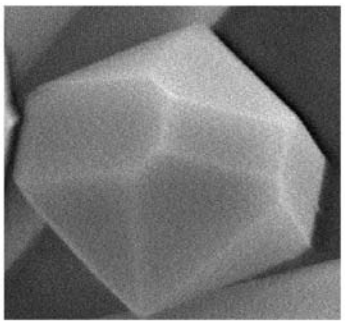

a single crystal

a twinned crystal

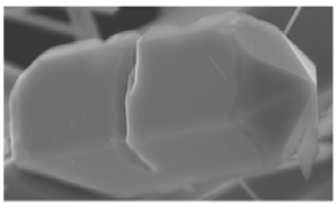

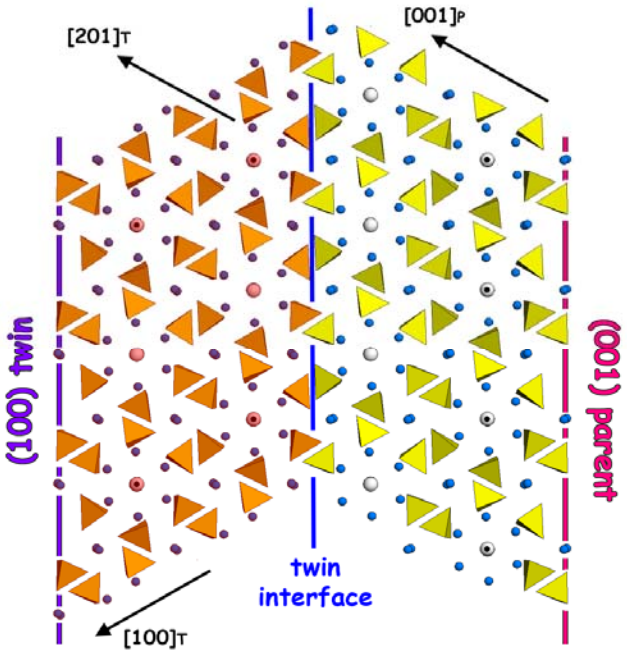

a twinned interface

Synopsis

The most frequent twin law of the monoclinic Hydroxyapatite crystal is examined. The structure of the resulting twinned interfaces are hypothesized and the twin energy for each interface is calculated. It results that the activation energy for the nucleation of a 3D twin can be hardly distinguished from the one needed to nucleate a single 3D crystal.